ELSEVIER

Journal of Power Sources 68 (1997) 726–729

JOURNAL OF POWER SOURCES

Rocking-chair batteries based on $LiMn_2O_4$ and V_6O_{13}

M.Y. Saïdi *, R. Koksbang, E.S. Saïdi, H. Shi, J. Barker

Valence Technology Inc., 301 Conestoga Way, Henderson, NV 89015, USA

Accepted 28 October 1996

Abstract

Lithium manganese oxide, $LiMn_2O_4$ and vanadium oxide, V_6O_{13}, have long been regarded as viable cathodes for rechargeable lithium batteries. The high operating voltage of $LiMn_2O_4$, 4 V versus Li, combined with the 2.3 V (versus Li/Li^+) average voltage of the V_6O_{13} system gives the possibility of a rocking-chair battery with a 1.5 V average operating voltage and good cycling capabilities. In this work, the feasibility of such a rocking chair is demonstrated. Electrochemical investigations were undertaken on cells incorporating a reference electrode. The corresponding rocking-chair cells exhibit good capacity retention and long-cycle life. © 1997 Elsevier Science S.A.

Keywords: Lithium batteries; Rocking-chair batteries, Vanadium oxide

1. Introduction

Among the transition metal oxides that are currently being evaluated as cathode materials for lithium batteries, V_6O_{13} and $LiMn_2O_4$ have received considerable attention [1–4]. This is primarily due to their high theoretical energy densities combined with excellent rechargeability and relative ease of preparation. The spinel phase $LiMn_2O_4$ is of particular interest because it can be used in conjunction with suitable carbon anode materials to produce the so-called 'rocking-chair' or 'lithium-ion technology' [5] batteries. These systems normally (but not exclusively) incorporate intercalation carbons (e.g. graphite or petroleum coke). The use of non-metallic lithium is expected to impart a significant safety advantage for these batteries. Alternative lithium-ion systems have also been suggested which exclude the use of carbon, and which use two different transition metal oxides as both lithium sink and source. For example, Plitcha and Behl [6,19] have described in detail the Li_xTiS_2/Li_xCoO_2 system. Although, highly lithiated vanadium oxide, $Li_xV_6O_{13}$, and $LiMn_2O_4$ are poor electronic conductors and addition of a conductive carbon is necessary to allow full utilization of the material, they can individually deliver sufficient energy for most applications.

Improvements in the reversible capacity of the $LiMn_2O_4$ and V_6O_{13} have been demonstrated by several workers through a clearer understanding of the parameters controlling their electrochemical behavior. The conditions of synthesis and control of the material structure have, in particular, received significant attention. Ohzuku et al. [7], and Tarascon et al. [8] have reported extensively on the electrochemical performance of $LiMn_2O_4$ and its dependency on the precise preparative conditions. On the other hand, Spurdens et al. among other workers [9–11] report on the synthesis of V_6O_{13} and V_6O_{13+x} ($0<x<0.5$) and show that slightly oxygen rich vanadium oxide exhibited substantial lithium capacity and a good rechargeability. Specific capacities around 120 and 300 mAh/g for $LiMn_2O_4$ and V_6O_{13} were reported for materials cycled in cells with a lithium metal counter electrode [12,13].

2. Experimental

Vanadium oxide was prepared by thermal decomposition of ammonium metavanadate, NH_4VO_3, under a flow of nitrogen. The metavanadate was heated at a rate of 0.5 °C/min to 440 °C and held there for 2 h, then cooled at the same rate to room temperature. $Li_{1+x}Mn_2O_4$ was prepared by firing appropriate amounts of EMD (electrolytic manganese dioxide) and Li_2CO_3 (Aldrich, 99.9%) to 800 °C for 48 h in open air. The lithium concentration in the lithium manganese oxide material was analyzed by atomic absorption spectroscopy using an Instrumentation Laboratory 357 spectrophotometer and thermogravimetric analysis. The phase purity of the materials was investigated using a Siemens D5000 powder diffractometer with the Cu Kα radiation. The lattice constants were obtained from an iterative least-square fitting method

* Corresponding author. e-mail: 7634.3656@compuserve.com

PII S0378-7753(97)02527-5

compiled from the observed d-spacings and the material's respective space-groups using 'Pirum' refinement program [14]. No other crystalline phases were detected. The cubic unit-cell parameter obtained from the diffraction pattern for $LiMn_2O_4$ having a spinel structure with the space group $Fd3m$ was 8.227(2) Å. The values of the cell parameters for V_6O_{13} with a monoclinic cell with the space group $C2/m$ were $a = 11.92(3)$ Å, $b = 3.68(3)$ Å, $c = 10.099(3)$ Å and $\beta = 101.01°$. These parameters are in good agreement with literature data [11,15].

The cells consisted of $LiMn_2O_4$-based cathodes against V_6O_{13} electrodes. To determine the $LiMn_2O_4/V_6O_{13}$ cell balance, both electrodes were cycled individually under electrochemical voltage spectroscopy (EVS) conditions ((i.e. voltage step ± 10 mV, critical current density, $I_{lim} < 50$ μA/cm^2) versus a lithium metal anode between preset limits of 3.0 to 4.3 V for the $Li/LiMn_2O_4$ system and 3.0 to 1.8 V for the Li/V_6O_{13} system. Then, the active materials loading were adjusted so that their elcetrode capacities would be approximately matched. The electrolyte consisted of a solution of ethylene carbonate–dimethyl carbonate (EC–DMC) and 1 M $LiPF_6$ with an EC:DMC ratio of 66:34. The electrode area was 24 cm^2. The entire cell assembly was placed in a flexible encapsulation which was heat-sealed under vacuum. To deconvolute the individual electrode responses of both electrodes, cells incorporating a lithium reference electrode were made. Voltage traces were recorded using EVS. This technique yields information regarding structural phase changes and order/disorder phenomena [4,16,17]. The electrochemical measurements were conducted under thermostatic conditions at 23 °C, using either an Advantest R6142 precision voltage sink/source coupled to a HP Model HP3144A digital multimeter, or alternatively a Schlumberger Instruments Model 1286 electrochemical interface.

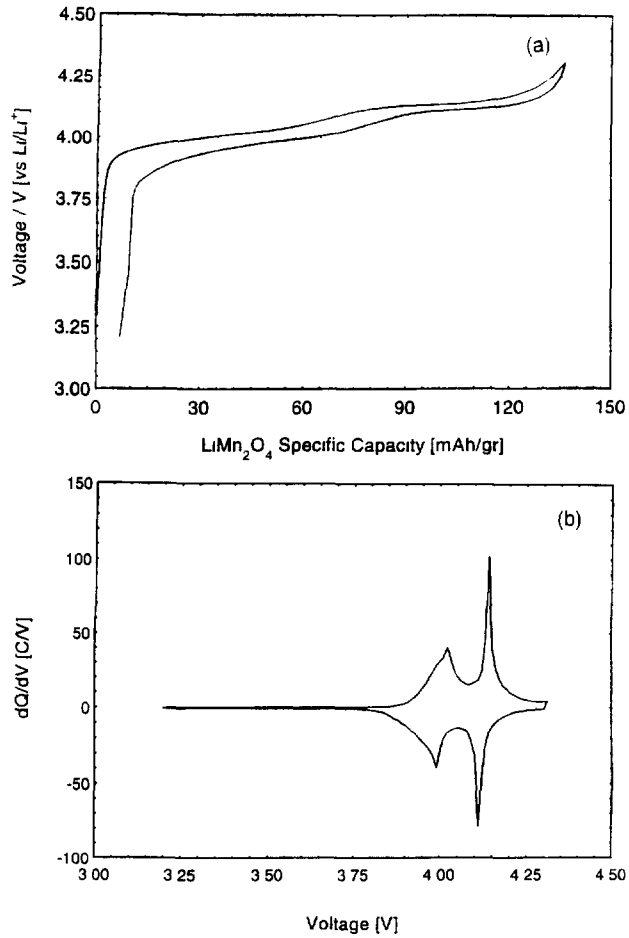

Fig. 1. (a) EVS voltage profile of an $Li/LiMn_2O_4$ cell; (b) corresponding EVS differential capacity plot.

3. Results and discussion

3.1. The $Li/LiMn_2O_4$ system

The EVS voltage profile and associated differential capacity data for the parent $Li_xMn_2O_4$ material are shown in Fig. 1(a) and (b), respectively. The voltage data should be looked upon as pseudo open-circuit data since the EVS experimental parameters essentially remove all cell voltage corrections associated with the cell IR drop or diffusion overvoltages within the electrochemical cell. The voltage profile shows the normal features normally associated with the parent $Li_xMn_2O_4$, i.e. the two distinctive voltage plateaus centered around 3.95 and 4.15 V versus Li/Li^+, respectively. As previously reported these voltage plateaus are associated with the two intercalation steps for the inserted lithium ions into the host lattice [4,7]. The small level of hysteresis present between the oxidative–reductive waves shown in this figure is indicative of the low overvoltage associated with the insertion/de-insertion processes within the particular voltage range.

The differential capacity profiles give information relating not only to the particular energetics for the intercalation reactions but also data pertaining to the order/disorder phenomenon in these materials. Fig. 1(b) shows that the parent spinel material generates two sharp differential capacity peaks with small overlap between the anodic (above the axis) and cathodic waves. This behavior is typical for the spinel intercalation.

3.2. The Li/V_6O_{13} system

For the Li/V_6O_{13} system, essentially three voltage plateaus are present centered around 2.75, 2.55 and 2.10 V versus Li/Li^+ in Fig. 2(a) and (b). These plateaus represent the sequential filling of non-equivalent sites that are present within the structure. The sharp peak centered at ~2.10 V (versus Li/Li^+) is typical of a two-phase region in Fig. 2(b). The corresponding feature in the voltage profile shows an e.m.f. which is capacity independent. The shape of the other sets of peaks represent complex phase transitions that vanadium oxide undergoes upon lithium uptake. The discharge

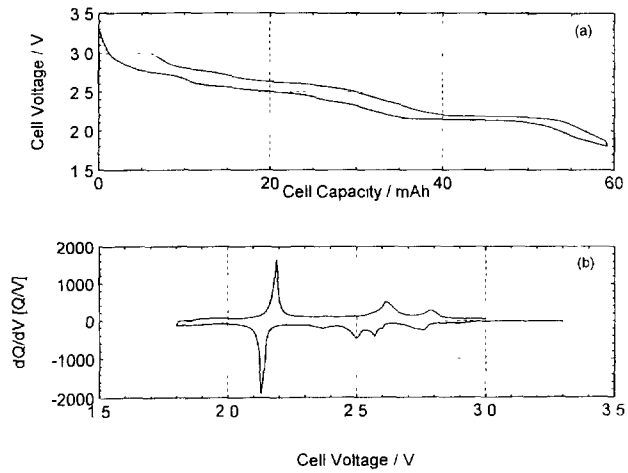

Fig 2 (a) EVS voltage profile of an Li/V_6O_{13} cell; (b) corresponding EVS differential capacity plot.

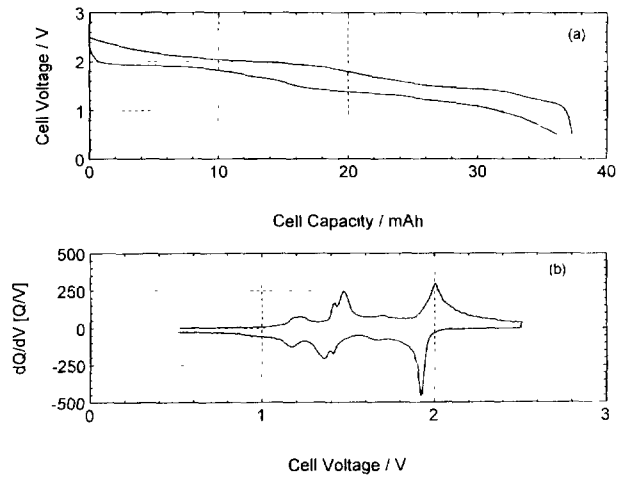

Fig 4. (a) EVS voltage trace of an $LiMn_2O_4/V_6O_{13}$ cell; (b) corresponding EVS differential capacity plot.

capacity for this cell corresponds to an active material utilization of 310 and 110 mAh/g for V_6O_{13} and $LiMn_2O_4$, respectively, demonstrating the high utilization of the material in accordance with previously reported data from this group and elsewhere [11,18].

3.3. The $LiMn_2O_4/V_6O_{13}$ system

Fig. 3 shows the voltage profile of an $LiMn_2O_4/V_6O_{13}$ cell cycled at a 0.25 mA/cm^2 rate between 0.5 and 2.5 V. The individual voltage profiles for each electrode versus the lithium reference electrode are indicated by arrows. It is seen that the features associated with the cell's voltage profile are dominated by those of the vanadium oxide electrode. The latter features three plateaus between 3 and 1.8 V (versus Li/Li^+). The characteristic features of the $LiMn_2O_4$ electrode are preserved. From the voltage profile, an average discharge voltage of 1.5 V may be estimated. Fig. 4(a) and (b) shows the EVS voltage profile and associated differential capacity data for a two-electrode configuration cell. The small level

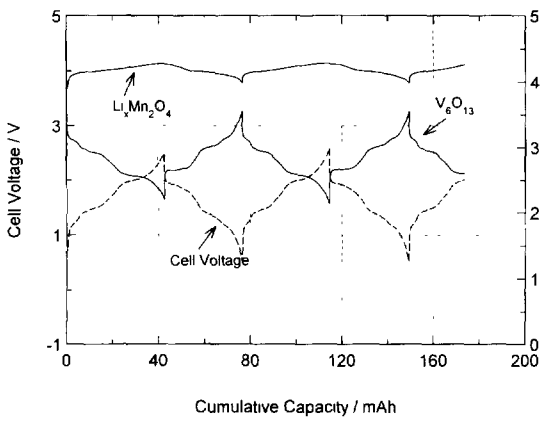

Fig 3. Voltage profile of an $LiMn_2O_4/V_6O_{13}$ cell. The individual responses from both electrodes are indicated by arrows.

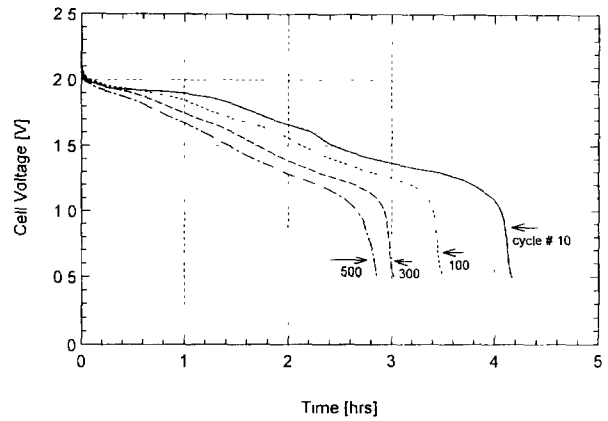

Fig. 5. Evolution of the voltage profile during cell discharge at different stages of the cycle life.

of hysteresis is indicative of the low overvoltage associated with the insertion/de-insertion processes within the particular voltage range. The differential capacity plot emphasizes the subtle features in the voltage profile and shows at least five reversible peaks. The complexity of the trace is dominated by the combination of the various phase transitions that V_6O_{13} and $LiMn_2O_4$ undergo upon lithium intercalation.

Cells based on $LiMn_2O_4$ and V_6O_{13} were cycled under constant-current conditions between voltage limits of 0.5 and 2.5 V and at current densities of 0.25 mA/cm^2 for both discharge and charge. Fig. 5 shows the discharge voltage trace at different stages of the cycle life. After 500 cycles, 70% of the initial capacity is still retained. The extended cycle life, see Fig. 6, highlights the excellent reversibility of lithium insertion and extraction in both the vanadium and manganese oxide systems with initial specific capacities of 310 and 122 mAh/g for V_6O_{13} and $LiMn_2O_4$, respectively, corresponding to a reversible faradaic yield of 5.7 Li per V_6O_{13} and 0.82 Li per Mn_2O_4.

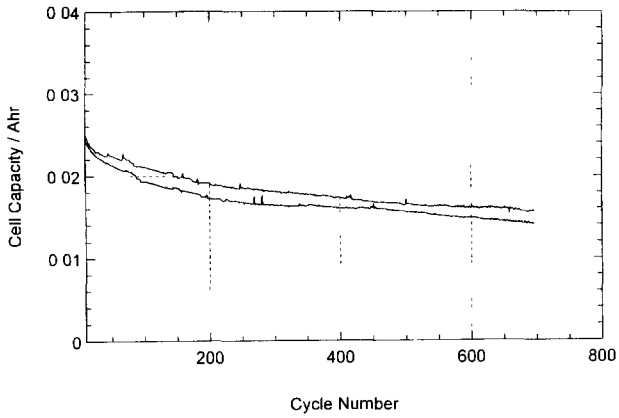

Fig 6 Discharge capacity of two $LiMn_2O_4/V_6O_{13}$ cells as a function of cycle number. $I_d = I_c = 0.25$ mA/cm^2

4. Conclusions

The concept of rocking-chair cells based on V_6O_{13} and $LiMn_2O_4$ has been demonstrated. Both materials are easy to prepare and individually show excellent reversibility towards lithium insertion and extraction. This system exhibits a good capacity retention with cycle life. Such a rocking-chair system, with a 1.5 V average voltage may be an attractive alternative in applications where a moderate energy density combined with an outstanding cycling capability are at a premium. Initial calculations have shown that a gravimetric and volumetric energy densities of 70 Wh/kg and 170 Wh/l could be achieved.

References

[1] D.W. Murphy, P.A. Christian, J.N. Carides and F.J. Disalvo, *Proc. Conf. on Fast-ion Transport in Solids, Lake Geneva, WI, USA, 21–25 May, 1979*, Paper No. I-M.
[2] D.W. Murphy, J.N. Carides, F.J. Disalvo and J.V. Waszcak, *Mater. Res. Bull., 13* (1978) 1395.
[3] M. Thackeray, P. Johnson, L. de Picciotto, P.G. Bruce and J.B. Goodenough, *Mater. Res. Bull., 19* (1984) 179.
[4] M.Y. Saidi, J. Barker and R. Koksbang, *Electrochim. Acta, 41* (1996) 199.
[5] D. Guyomard and J.M. Tarascon, *J. Electrochem. Soc., 139* (1992) 937.
[6] E.J. Plitcha and W.K. Behl, *J. Electrochem. Soc., 140* (1993) 46.
[7] H. Ohzuku, M. Kitagawa and T. Hirai, *J. Electrochem. Soc., 137* (1990) 769.
[8] J. Tarascon, E. Wang, F. Shokooki, W. McKinnon and S. Colson, *J. Electrochem. Soc., 138* (1991) 2859.
[9] P.C. Spurdens, J. Drennan, J.R. Owen, B.C.H. Steele, J.M. Gonzales-Calbet and D.A. Jefferson, *Solid State Ionics, 5* (1981) 331.
[10] P.C. Spurdens and B.C.H. Steele, *Solid State Ionics, 21* (1986) 151.
[11] J. Barker, E.S. Saidi and M.Y. Saidi, *Electrochim. Acta 40* (1995) 949.
[12] M.Y. Saidi and J. Barker, *Solid State Ionics, 78* (1995) 169.
[13] M.Y. Saidi, R. Koksbang and J. Barker, *J. Power Sources*, (1996) in press.
[14] P.E. Werner, *Arkiv Kemi, 31* (1969) 513.
[15] G. Pistoia and G. Wang, *Solid State Ionics, 66* (1993) 135.
[16] A.H. Thompson, *Phys. Rev. Lett., 23* (1978) 1511.
[17] J. Barker, *Synth. Met., 32* (1989) 43.
[18] K. West, B. Zachau-Christiansen, T. Jacobsen and S. Atlung, *Electrochim. Acta, 28* (1983) 1829.
[19] E. Ferg, R.J. Gummow, A. de Kock and M.M. Thackeray, *J. Electrochem. Soc., 141* (1994) L147–L150.